

Transparent organic field-effect transistors with polymeric source and drain electrodes fabricated by inkjet printing

X.-H. Zhang, S. M. Lee, B. Domercq, and B. Kippelen

Citation: *Appl. Phys. Lett.* **92**, 243307 (2008); doi: 10.1063/1.2940232

View online: <http://dx.doi.org/10.1063/1.2940232>

View Table of Contents: <http://apl.aip.org/resource/1/APPLAB/v92/i24>

Published by the [American Institute of Physics](#).

Related Articles

Analysis of micro-Raman spectra combined with electromagnetic simulation and stress simulation for local stress distribution in Si devices

Appl. Phys. Lett. **101**, 243511 (2012)

The Maxwell-Wagner model for charge transport in ambipolar organic field-effect transistors: The role of zero-potential position

Appl. Phys. Lett. **101**, 243302 (2012)

Stable n-channel metal-semiconductor field effect transistors on ZnO films deposited using a filtered cathodic vacuum arc

Appl. Phys. Lett. **101**, 243508 (2012)

Role of barrier structure in current collapse of AlGaIn/GaN high electron mobility transistors

Appl. Phys. Lett. **101**, 243506 (2012)

The Maxwell-Wagner model for charge transport in ambipolar organic field-effect transistors: The role of zero-potential position

APL: Org. Electron. Photonics **5**, 267 (2012)

Additional information on *Appl. Phys. Lett.*

Journal Homepage: <http://apl.aip.org/>

Journal Information: http://apl.aip.org/about/about_the_journal

Top downloads: http://apl.aip.org/features/most_downloaded

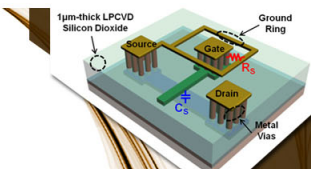
Information for Authors: <http://apl.aip.org/authors>

ADVERTISEMENT

AIP | Applied Physics
Letters


**EXPLORE WHAT'S
NEW IN APL**

SUBMIT YOUR PAPER NOW!



**SURFACES AND
INTERFACES**

Focusing on physical, chemical, biological, structural, optical, magnetic and electrical properties of surfaces and interfaces, and more...



**ENERGY CONVERSION
AND STORAGE**

Focusing on all aspects of static and dynamic energy conversion, energy storage, photovoltaics, solar fuels, batteries, capacitors, thermoelectrics, and more...

Transparent organic field-effect transistors with polymeric source and drain electrodes fabricated by inkjet printing

X.-H. Zhang, S. M. Lee, B. Domercq, and B. Kippelen^{a)}

Center for Organic Photonics and Electronics (COPE), School of Electrical and Computer Engineering, Georgia Institute of Technology, Atlanta, Georgia 30332, USA

(Received 8 April 2008; accepted 10 May 2008; published online 19 June 2008)

Transparent organic field-effect transistors based on pentacene were fabricated on indium tin oxide (ITO)-coated glass using ITO as the gate electrode, Al_2O_3 grown by atomic layer deposition as the gate insulator, and an inkjet-printed conducting polymer poly(3,4-ethylenedioxythiophene):poly(4-styrenesulphonate) as the source and drain electrodes. The transistors combine an overall high transmittance (84% in the channel and 78% through source/drain electrodes) in the visible region, a field-effect mobility value of $0.3 \text{ cm}^2/\text{V s}$, a threshold voltage of -0.2 V , a subthreshold slope of 0.9 V/decade , and an on/off current ratio of 10^5 . © 2008 American Institute of Physics. [DOI: 10.1063/1.2940232]

Organic field-effect transistors (OFETs) have recently gained great interest as building blocks for electronic applications that require low-cost, large-area, and potentially flexible form-factors. Some examples of these applications are radio-frequency identification tags,¹ drivers for electronic paper,² and driving circuits for flat panel displays.³ When processed into thin films, organic electronic materials can be used to build transparent transistors, benefiting from their weak absorbance in the visible spectrum. Invisible electronic circuits based on transparent transistors are potentially important for the applications requiring transparency, such as bendable heads-up display devices, see-through structural health monitors, and sensors.^{4–8} In backlit display devices, for example, transparent active-matrix circuits can increase the aperture ratio and operation lifetime.

Most transparent thin-film transistors (TFTs) use thin-film inorganic oxides as semiconducting and conducting layers.^{9–12} Although a mobility higher than $120 \text{ cm}^2/\text{V s}$ has been achieved from these oxides,¹¹ their mechanical properties are not compatible with flexible electronic devices. In addition to oxide-based TFTs, transistors based on single-wall carbon nanotubes (SWNTs) as both conductors and semiconductors also show great transparency.^{12,13} However, the on/off current ratio of these transistors is usually very low and varies with channel length.^{12–15} Semitransparent OFETs using pentacene as channel materials were reported with an overall transmittance of 25%–30%.¹⁶ The low transmittance was due to a high absorption from NiO_x used for the source (S) and drain (D) electrodes. Recent work also demonstrated transparent pentacene-based OFETs with SWNTs as electrodes patterned by transfer printing.¹⁷ However, unlike conductive polymers, SWNTs cannot be directly printed by inkjet printing, by screen printing, or by thermal laser printing. Conductive polymers, such as highly doped polyaniline and poly(3,4-ethylenedioxythiophene):poly(4-styrenesulphonate) (PEDOT:PSS), are attractive as transparent electrodes due to their ability to be processed from solution easily using standard printing techniques.

In this letter, we report the fabrication of high-performance transparent OFETs based on pentacene using PEDOT:PSS patterned by inkjet printing as the source and drain electrodes. A 200 nm thick film of Al_2O_3 was grown on indium tin oxide (ITO)-coated glass substrate (also serving as the gate) by atomic layer deposition (ALD), a technology that provides thin, high-quality films even on rough surfaces, as the gate dielectric material.¹⁸

Transistors were fabricated on ITO-coated glass substrates (Colorado Concept Coatings, $60 \Omega/\text{sq.}$), and ITO served as a gate electrode. A 200 nm thick Al_2O_3 film, served as a gate insulator, was deposited at 100°C using a Savannah100 ALD system from Cambridge Nanotech Inc. With a dielectric constant of 7.5 ± 0.2 at 1 kHz, the Al_2O_3 gate insulator yields a high capacitance density with a value of 32.7 nF/cm^2 . Despite a large root-mean-square (rms) roughness of 1.2 nm from the ITO-coated glass substrate, the leakage current density of Al_2O_3 at an applied field of 2 MV/cm was less than 100 nA/cm^2 when measured over a contact area of 0.016 cm^2 . The detailed growth conditions and characterization of Al_2O_3 gate insulators have been published elsewhere.¹⁸

Transparent OFETs were fabricated using a top-contact geometry, as illustrated in Fig. 1. Before the deposition of pentacene, ITO-coated glass substrates with Al_2O_3 gate insulators were dipped into a 5 mM toluene solution of octadecyltrichlorosilane (OTS) in a N_2 -filled glove box for 24 h to grow a uniform self-assembled monolayer on the Al_2O_3 layer. Then, a 50 nm thick layer of pentacene (Aldrich) purified by gradient zone sublimation was deposited at a vacuum level of $2 \times 10^{-8} \text{ Torr}$ at a deposition rate of 0.3 Å/s , as measured by a quartz crystal monitor. The sub-

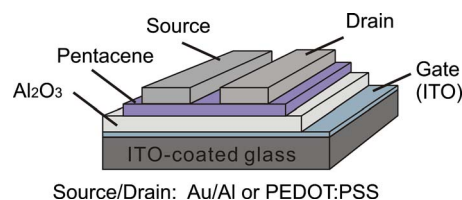


FIG. 1. (Color online) Schematic diagram of the OFET device geometry fabricated on ITO-coated glass substrates.

^{a)} Author to whom correspondence should be addressed. Tel.: 404-385-5163. FAX: 404-385-5162. Electronic mail: kippelen@gatech.edu.

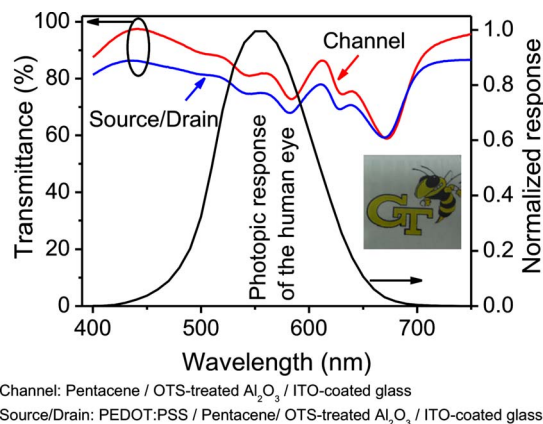


FIG. 2. (Color online) Left axis: optical transmission spectra through both the channel and the PEDOT:PSS source/drain electrodes of the transparent pentacene OFETs on ITO-coated glass; right axis: photopic response of the human eye. Inset: optical image of several arrays of transistors with printed PEDOT:PSS electrodes positioned above some printed text on paper to illustrate the degree of optical transparency.

strates were held at room temperature during deposition. After the pentacene deposition, some substrates were exposed to air and source/drain electrodes were fabricated by inkjet-printing PEDOT:PSS. The rest substrates were kept in the deposition chamber and a 40 nm thick Au film (capped with a 100 nm thick Al film) were deposited through a shadow mask to define source and drain electrodes on these control samples.

PEDOT:PSS (Baytron F HC, conductivity >150 S/cm) was printed in air using a DMP-2831 inkjet printer from DimatixTM. To improve its conductivity and surface wetting properties,¹⁹ PEDOT:PSS was mixed with dimethyl sulfoxide (DMSO) (10:1 by volume), followed by sonication for 10 min. The addition of DMSO also helped in preventing nozzle clogging problems. A drop spacing of 20 μm was chosen to provide a good droplet overlap while minimizing droplet flow and aggregation. The nozzle was heated to 30 $^\circ\text{C}$ to maintain a consistent temperature with the substrate held at room temperature. The drop frequency was adjusted to 5 kHz to yield optimized drying speed and drop spacing. After printing of the electrodes, the samples were transferred into a N_2 -filled box where electrical testing was carried out.

A Cary 5e UV-visible-near infrared spectra photometer was used to measure the optical transmission spectra through both the channel and the PEDOT:PSS source/drain electrodes of the transparent pentacene OFETs in the visible region between 400 and 750 nm (see Fig. 2). A piece of ITO-coated glass with ITO removed by wet etching was used as a reference sample. The transmission spectrum through the channel area reflects the optical loss and interference from the pentacene film, the OTS-treated Al_2O_3 and the ITO film, as seen in Fig. 1. The spectrum through the contact area also includes the effect from the additional layer of PEDOT:PSS used as electrodes. The 200 nm thick Al_2O_3 gate insulator layer and the PEDOT:PSS electrodes (~ 90 – 120 nm) are both highly transparent (transmittance $>80\%$) in the visible spectral region. The absorption of the device in the visible region is mostly from the 50 nm thick pentacene films, and it occurs in the red region at 668 nm. However, the maximum absorption from pentacene at 668 nm has negligible influence on human vision, as shown in Fig. 2. The transmittance, averaged in the visible region from 400 to 750 nm, is 84%

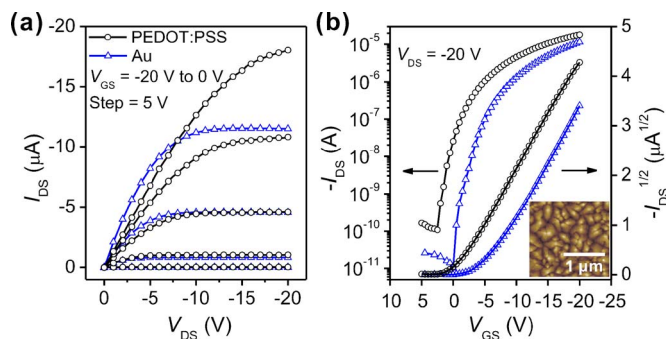


FIG. 3. (Color online) Comparison of output characteristics (a) and transfer characteristics (b) of pentacene OFETs ($W=2000$ μm , $L=200$ μm) with PEDOT:PSS and Au as source and drain electrodes. Inset: AFM image of pentacene on OTS treated Al_2O_3 deposited on ITO-coated glass.

through the channel region and is slightly decreased to 78% in the area of source/drain electrodes with the additional layer of PEDOT:PSS, demonstrating the high transparency of PEDOT:PSS electrodes. Transmittance could be further increased with thinner pentacene layers. The inset in Fig. 2 shows an image of several arrays of printed PEDOT:PSS electrodes on glass positioned above a reference background image to illustrate the level of optical transparency.

Figure 3 compares the output [Fig. 3(a)] and transfer characteristics [Fig. 3(b)] of pentacene OFETs with printed PEDOT:PSS and evaporated Au as source/drain electrodes, respectively. The two types of devices had an identical geometry with a channel length $L=200$ nm and a channel width $W=2000$ μm . The electrical measurements of the pentacene OFETs were performed in a N_2 -filled glovebox ($\text{O}_2, \text{H}_2\text{O} < 0.1$ ppm) using an Agilent E5272A source/monitor unit. The inset in Fig. 3(b) shows a typical atomic force microscopy (AFM) image (2×2 μm^2) of the pentacene films on OTS-treated Al_2O_3 with well-ordered crystalline domains and an average grain size of 0.2–0.5 μm . The values of the mobility and those of the threshold voltage V_T in the saturation regime with drain-source voltage V_{DS} of -20 V were extracted using a metal-oxide-semiconductor FET square-law model. Also extracted from the transfer characteristics were subthreshold slopes S , turn-on voltages V_{TO} , and on/off current ratios $I_{on/off}$. The electrical parameters are summarized and compared in Table I.

As we described earlier, the device with PEDOT:PSS was exposed to ambient condition for printing and also exposed to the water and other chemicals present in the PEDOT:PSS solution. The effect of the possible contamination during processing of the PEDOT:PSS electrodes is reflected in the transfer characteristic with a smaller value of the turn-on voltage ($V_{TO}=-2.5$ V), a reduced value of the threshold voltage ($V_T=-0.2$ V), and a larger subthreshold slope ($S=0.9$ V/decade) compared to those obtained from

TABLE I. Summary of the electrical parameters for pentacene OFETs ($W=2000$ μm , $L=200$ μm) with different source/drain (S/D) electrodes. μ for field-effect mobility, V_T for threshold voltage, V_{TO} for turn-on voltage, S for subthreshold slope, and $I_{on/off}$ for on/off current ratio.

S/D electrodes	μ (cm ² /V s)	V_{TO} (V)	V_T (V)	S (V/decade)	$I_{on/off}$
PEDOT:PSS	0.30	-2.5	-0.2	0.9	1×10^5
Au	0.32	0.0	-5.5	0.6	1×10^6

devices with a pristine pentacene film and Au electrodes ($V_{TO}=0$, $V_T=-5.5$ V and $S=0.6$ V/decade). These effects have been attributed to the creation of acceptorlike states in the pentacene film after exposure to oxygen and moisture.²⁰ This also explains the increased off-state current which leads to a slightly lower on/off ratio (10^5) with PEDOT:PSS electrodes.

It has been observed that moisture also has an influence on the Au/pentacene interface and cause a decreased mobility during device operation.^{20,21} However, with PEDOT:PSS as S/D electrodes in our work, the pentacene OFET shows a comparable mobility $\mu=0.3$ cm²/V s and even a higher on-current $I_{on}=18$ μ A in comparison with devices with Au electrodes ($\mu=0.32$ cm²/V s, $I_{on}=11$ μ A). This can be attributed to the smaller injection barrier (0.25 eV) at the PEDOT:PSS/pentacene interface compared with that at the Au/pentacene interface (0.85 eV) despite the very similar work functions (5 eV) of the two electrodes.²²

In conclusion, transparent OFETs have been fabricated using inkjet-printed PEDOT:PSS as top source and drain electrodes and ALD-deposited Al₂O₃ as the gate insulator. With a high averaged transmittance (84% in the channel and 78% through source/drain electrodes) in the visible region, these OFETs also exhibit a performance similar or slightly better than that of reference OFETs with Au electrodes. PEDOT:PSS has an excellent transparency and solution processibility, and its conductivity can be further improved by chemical doping. Al₂O₃ deposited at 100 °C by ALD has great dielectric properties even on substrates with a large roughness, which will become especially critical for most flexible substrates of interest.

This material is based upon work supported in part by the STC Program of the National Science Foundation under Agreement No. DMR-0120967, by the Office of Naval Research. This work was performed in part at the Microelectronics Research Center at Georgia Institute of Technology, a member of the National Nanotechnology Infrastructure Network, which is supported by NSF (Grant No. ECS-03-35765).

- ¹V. Subramanian, J. M. J. Frechet, P. C. Chang, D. C. Huang, J. B. Lee, S. E. Moles, A. R. Murphy, D. R. Redinger, and S. K. Volkman, *Proc. IEEE* **93**, 1330 (2005).
- ²G. H. Gelinck, H. E. A. Huitema, E. van Veenendaal, E. Cantatore, L. Schrijnemakers, J. B. P. H. van der Putten, T. C. T. Geuns, M. Beenhakkers, J. B. Giesbers, B.-H. Huisman, E. J. Meijer, E. M. Benito, F. J. Touwslager, A. W. Marsman, B. J. E. van Rens, and D. M. de Leeuw, *Nat. Mater.* **3**, 106 (2004).
- ³L. Zhou, A. Wanga, S.-C. Wu, J. Sun, S. Park, and T. N. Jackson, *Appl. Phys. Lett.* **88**, 083502 (2006).
- ⁴S. R. Forrest, *Nature (London)* **428**, 911 (2004).
- ⁵R. H. Reuss, B. R. Chalamala, A. Moussessian, M. G. Kane, A. Kumar, D. C. Zhang, J. A. Rogers, M. Hatalis, D. Temple, G. Moddel, B. J. Eliasson, M. J. Estes, J. Kunze, E. S. Handy, E. S. Harmon, D. B. Salzman, J. M. Woodall, M. A. Alam, J. Y. Murthy, S. C. Jacobsen, M. Olivier, D. Markus, P. M. Campbell, and E. Snow, *Proc. IEEE* **93**, 1239 (2005).
- ⁶K. Nomura, H. Ohta, A. Takagi, T. Kamiya, M. Hirano, and H. Hosono, *Nature (London)* **432**, 488 (2004).
- ⁷K. Nomura, H. Ohta, K. Ueda, T. Kamiya, M. Hirano, and H. Hosono, *Science* **300**, 1269 (2003).
- ⁸J. F. Wager, *Science* **300**, 1245 (2003).
- ⁹P. Gorrn, M. Sander, J. Meyer, M. Kroeger, E. Becker, H.-H. Johannes, W. Kowalsky, and T. Riedl, *Adv. Mater. (Weinheim, Ger.)* **18**, 738 (2006).
- ¹⁰E. M. C. Fortunato, P. M. C. Barquinha, A. C. M. B. G. Pimentel, A. M. F. Goncalves, A. J. S. Marques, L. M. N. Pereira, and R. F. P. Martins, *Adv. Mater. (Weinheim, Ger.)* **17**, 590 (2005).
- ¹¹L. Wang, M.-H. Yoon, G. Lu, Y. Yang, A. Facchetti, and T. J. Marks, *Nat. Mater.* **5**, 893 (2006).
- ¹²Q. Cao, S.-H. Hur, Z.-T. Zhu, Y. Sun, C. Wang, M. A. Meitl, M. Shim, and J. A. Rogers, *Adv. Mater. (Weinheim, Ger.)* **18**, 304 (2006).
- ¹³E. Artukovic, M. Kaempgen, D. S. Hecht, S. Roth, and G. Gruner, *Nano Lett.* **5**, 757 (2005).
- ¹⁴S.-H. Hur, C. Kocabas, A. Gaur, O. O. Park, M. Shim, and J. A. Rogers, *J. Appl. Phys.* **98**, 114302 (2005).
- ¹⁵S.-H. Hur, M.-H. Yoon, A. Gaur, M. Shim, A. Facchetti, T. J. Marks, and J. A. Rogers, *J. Am. Chem. Soc.* **127**, 13808 (2005).
- ¹⁶D. K. Hwang, C. S. Kim, J. M. Choi, K. Lee, J. H. Park, E. Kim, H. K. Baik, J. H. Kim, and S. Im, *Adv. Mater. (Weinheim, Ger.)* **18**, 2299 (2006).
- ¹⁷Q. Cao, Z.-T. Zhu, M. Lemaitre, M.-G. Xia, M. Shim, and J. A. Rogers, *Appl. Phys. Lett.* **88**, 113511 (2006).
- ¹⁸X.-H. Zhang, B. Domercq, X. Wang, S. Yoo, T. Kondo, Z. L. Wang, and B. Kippelen, *Org. Electron.* **8**, 718 (2007).
- ¹⁹J. A. Lim, J. H. Cho, Y. D. Park, D. H. Kim, M. Hwang, and K. Cho, *Appl. Phys. Lett.* **88**, 082102 (2006).
- ²⁰D. Knipp, A. Benor, V. Wagner, and T. Muck, *J. Appl. Phys.* **101**, 044504 (2007).
- ²¹G. Gu and M. G. Kane, *Appl. Phys. Lett.* **92**, 053305 (2008).
- ²²N. Koch, A. Elschner, J. P. Rabe, and R. L. Johnson, *Adv. Mater. (Weinheim, Ger.)* **17**, 330 (2005).